

DETECTION OF VERTICAL CRACKS IN CARBON FIBER COMPOSITES USING AN INFRARED LINE SCANNER

Jussi Varis

Department of Physics
University of Helsinki
P. O. Box 9, FIN-00014 University of Helsinki
Helsinki, Finland

INTRODUCTION

Vertical cracks are among the most problematic types of defects from the thermal nondestructive testing (NDT) point of view. Nowadays, the fast thermal inspection techniques most commonly utilize infrared cameras and pulsed heating provided by flash lamps. The flash lamps illuminate the whole surface of a sample, and the resulting heat flow is mostly perpendicular to the surface. Therefore, the heat signature caused by the vertical cracks may be very small, and the cracks may avoid detection.

Techniques like "mirage" [1] and "flying spot" [2] have been utilized for crack detection successfully. Another possible solution might be the use of line heating and an infrared line scanner demonstrated earlier by Hartikainen [3]. This method has been used earlier for detecting delaminations [4] and impact damages [5] in carbon fiber composites. In this paper, the work is continued by applying the method for crack detection in unidirectional carbon fiber composites. The applicability of the method is based on the lateral heat flow generated by the moving line heat source. A vertical crack parallel to the line source will stop or hinder the heat flow, and a detectable heat signature should be formed. However, if the crack is perpendicular to the heating line, it will most probably stay undetected [6].

COMPUTATIONAL MODEL

The carbon fiber composite sample used in this study consists of nine unidirectional plies, each of which is 80 μm thick (Fig. 1). The laminate was covered from both sides with woven 2-D protective skins. The total thickness of the composite plate was approximately 800 μm . In the plate, several 20 mm long and 0.2 mm wide cuts were made to simulate vertical cracks reaching the sample surface. The cuts ranged from one to five plies in depth.

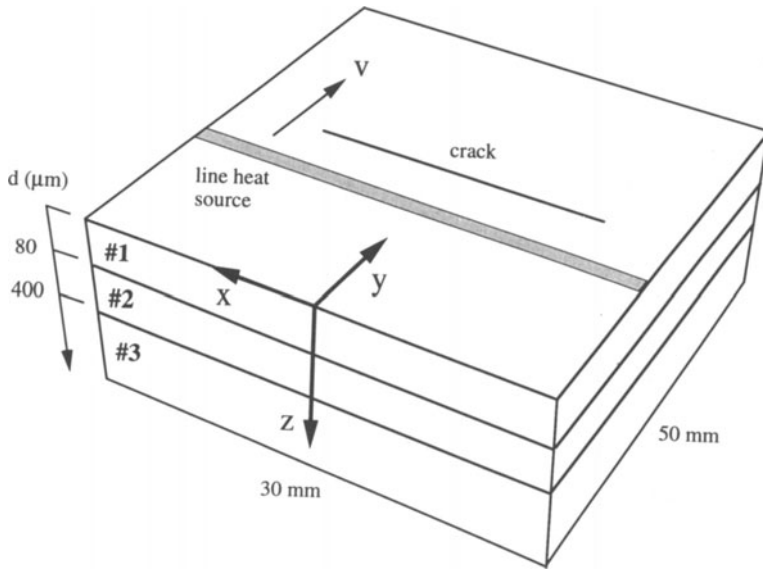


Fig. 1. A schematic drawing of the numerical model used in the calculations. The crack is parallel to the heating line.

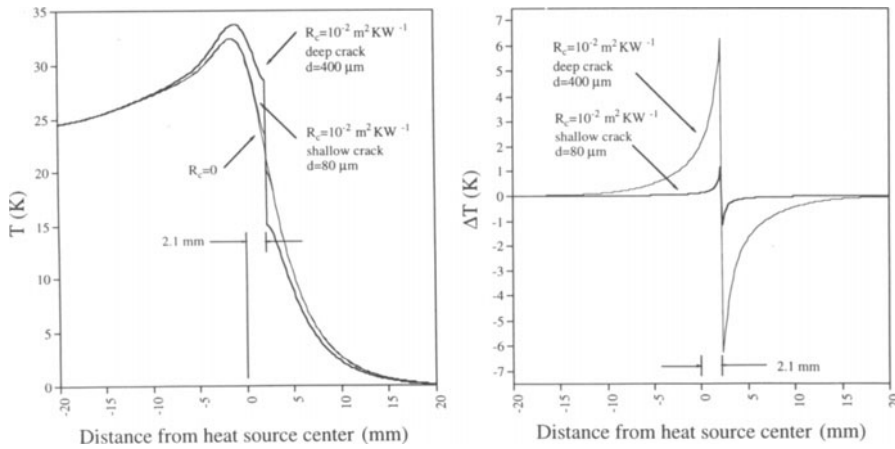


Fig. 2. a) The surface temperature profiles in the cases of a perfect sample, 80 μm deep surface crack, and 400 μm deep surface crack. b) The temperature difference profiles obtained by subtracting the curve with no defect from the curves with the cracks.

Table I. Thermal parameters used in the numerical computations

κ_v ($\text{W m}^{-1} \text{K}^{-1}$)	$\kappa_{x,z}$ ($\text{W m}^{-1} \text{K}^{-1}$)	ρ (kg m^{-3})	c ($\text{J kg}^{-1} \text{K}^{-1}$)
11.1	0.87	1400	935

Surface temperature distributions caused by the cracks were estimated with a finite difference numerical model. The sample was modelled with $20 \times 240 \times 15$ grid points corresponding to a physical sample size of $30 \text{ mm} \times 50 \text{ mm} \times 0.8 \text{ mm}$. The model was divided into three layers, which made it possible to study the effects of crack depth, d , on the surface temperature of the sample. The first layer consisted of the top ply. The second and the third layer had four plies each. Fiber orientation was implemented in the model by using two different thermal conductivity values depending on whether the coordinate direction was parallel to the fibers or perpendicular to them. In this case, the fiber orientation was chosen to be the y -direction, where a larger conductivity value was used, whereas in the x - and z -direction a smaller one was used (see Table I). The 20 mm long crack was simulated by using a thermal contact resistance values, $R_c = 10^{-2} \text{ m}^2\text{KW}^{-1}$, placed between grid points in the y -direction and forming a line in the x -direction. The sample was heated with a line source parallel to the crack, and the source was scanned in the y -direction with the velocity of $v = 2 \text{ mm/s}$. A very wide source of 5.7 mm was used with the heating power of 10 W .

The results of the calculations are shown in Fig. 2 a) and b). Fig. 2 a) shows the surface temperature profiles in cases of a perfect sample, a shallow crack ($d = 80 \mu\text{m}$), and a deep crack ($d = 400 \mu\text{m}$). The cracks can be seen as discontinuities 2.1 mm away from the heating line center; that is, where the leading edge of the heating line is. The deep crack stops the lateral net heat flow in the y -direction more efficiently causing a stronger effect on the surface temperature. In the case of the shallow crack, the effect is barely visible. This effect can be made clearer by subtracting the curve with no defect from the ones with the cracks. Fig. 2 b) shows the temperature difference profiles obtained this way. In both the cases, the maximum temperature difference is 1 K or bigger, and the cracks should be detectable. Both the temperature difference curves show a heat buildup on the first edge of the crack, whereas a sink can be seen in the second edge. This can be explained by observing that the heat flow is in the positive y -direction, and that the fiber orientation is the same. Thus, the fibers transfer the heat towards the crack, before the line source has reached the crack. When the line source is on the other side of the crack, the fibers conduct the heat away from the crack.

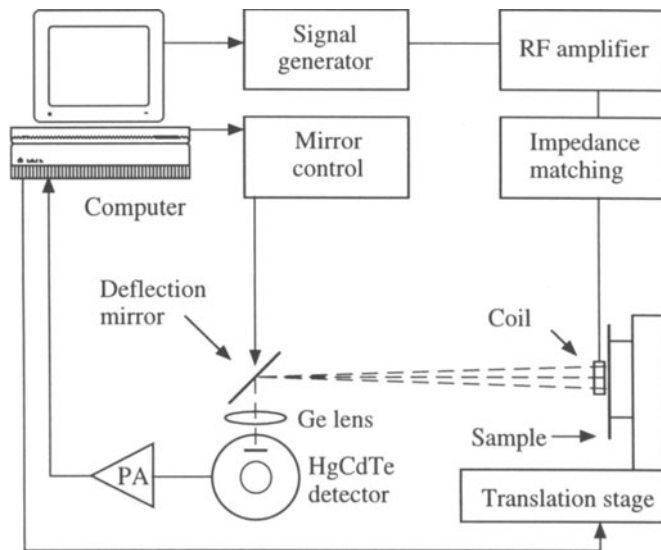


Fig.3. The measurement system.

EXPERIMENTAL SETUP

The measurements were made using an infrared line scanning measurement system (Fig. 3) described earlier by Lehtiniemi and Hartikainen [5]. The line heat source was generated with an radio frequency induction coil, which was 5.7 mm wide and 30 mm long. The estimated heating power on the sample surface was 10 W. The sample was moved perpendicularly towards the heating coil with a stepping motor, and simultaneously the surface temperature was monitored with an ac coupled MCT detector (area: $25\ \mu\text{m} \times 25\ \mu\text{m}$; wavelength region: 8-12 μm). With the help of a deflection mirror, the system was able to image the sample surface alongside the coil in 200 separate points. During the movement of the sample, 200 image lines were taken. With the lines combined, a 200×200 pixel pseudo color image was formed of the sample surface. The measurement time of one frame was 3.2 s. The whole measurement process was controlled with a microcomputer.

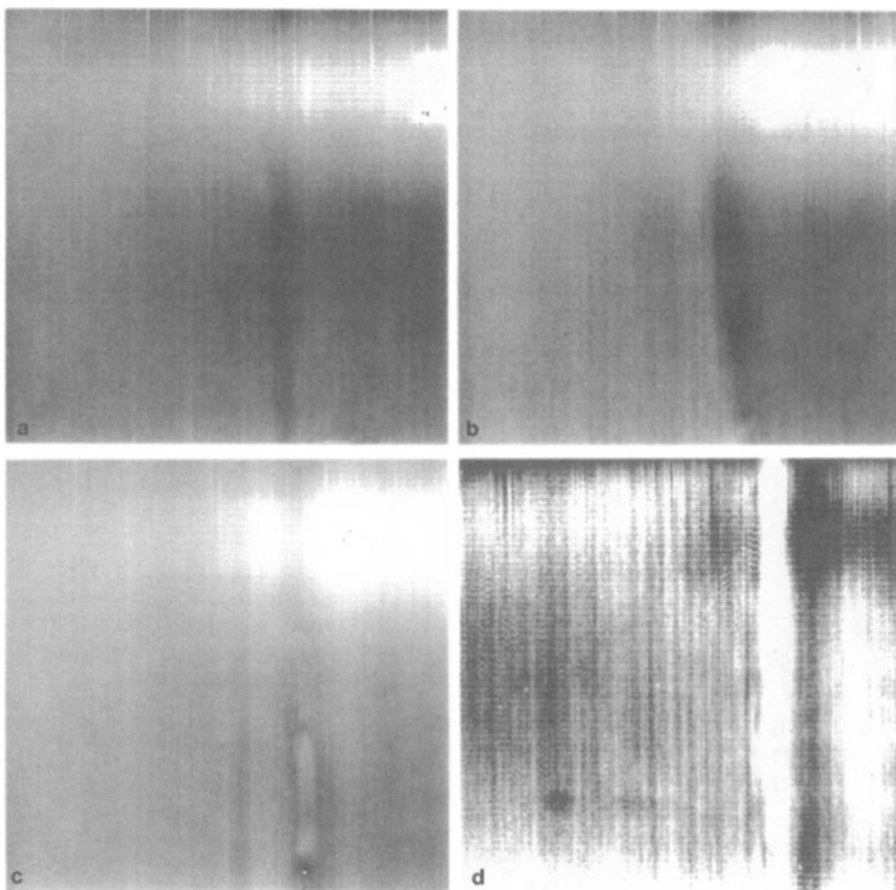


Fig. 4. a) A thermal image of a vertical crack in an unidirectional carbon fiber composite. The crack cuts the fibers in the first three plies ($240\ \mu\text{m}$). b) A thermal image of a vertical crack cutting the carbon fibers in the first four plies ($320\ \mu\text{m}$). c) A thermal image of a vertical crack cutting the carbon fibers in the first five plies ($400\ \mu\text{m}$). d) An enhanced thermal image showing two cracks perpendicular to each other. In all the cases, the imaged areas are $25\ \text{mm} \times 25\ \text{mm}$, and the width of the cracks are $200\ \mu\text{m}$.

RESULTS

Fig. 4 shows four thermal images obtained with the infrared line scanner. The imaged areas are 25 mm x 25 mm. The heating line was positioned vertically in the images, and it moved from left to right. In Figs. 4 a) - c) a series of cuts ranging from 3 plies to 5 plies in depth can be seen. In the case of 3 plies (Fig. 4 a), the crack is visible, but surface features like the texture of the protective skin are also very prominent in the image. Induction heating is sensitive to the distance of the coil from the surface of the sample. Therefore, areas that are higher than the rest of the surface heat up better, and as a result the image suffers from nonuniform heating effects. There is no evident heat buildup on the first edge of the crack as the numerical model predicts.

In Fig. 4 b) (four plies), the crack is clearer and its shape is visible. This time, there seems to be a heat buildup on the first edge and a sink on the second edge. However, the cooler area does not have the same shape as the crack, which suggests that there are factors involved in the image formation other than those discussed with the numerical model. In the case of 5 plies (Fig. 4 c), there can be seen inner structure in the saw cut. The damage is more serious than in the previous images, and delaminated areas can be detected. This time no heat buildup is evident. The last case (Fig. 4 d) shows an image of two cracks, one of which is in the vertical direction in the image, and the other which is in the horizontal direction in the image. The heating line is again positioned vertically. The crack parallel to the heating line is clearly visible, whereas the other one can barely be detected. After image enhancement, faint traces (black) of the horizontal crack can be seen in front of the vertical crack in the lower part of the image. This result supports earlier conclusions [6] that cracks perpendicular to the heating line do not hinder the lateral heat flow enough for the cracks to be easily detected.

CONCLUSIONS

Scanned line heating combined with an infrared line scanner provides a possible solution for detecting vertical cracks in unidirectional carbon fiber composites. In this study, 0.2 mm wide saw cuts with the depth of three plies or deeper were detected. Cuts that do not reach the sample surface, or cuts that are shallower than three plies could not be detected. Also, cuts that were perpendicular to the heating line remained undetected.

ACKNOWLEDGEMENT

Mr. I. Savonije from FinnAvicom Oy is gratefully acknowledged for his pleasant cooperation and for providing the carbon fiber composite sample.

REFERENCES

1. J.Rantala, J. Jaarinen, and J. Hartikainen, *Appl. Phys. A* 50, 465 (1990)
2. Y.Q. Wang, P. K. Kuo, L.D. Favro, and R. L. Thomas, in *Review Of Progress in QNDE*, Vol. 9A, eds. D.O. Thompson and D.E. Chimenti (Plenum Press, New York, 1990), p. 511
3. J. Hartikainen, *Rev. Sci. Instrum.* 60, 1334 (1989)
4. J. Varis, J. Rantala, and J. Hartikainen, *NDT&E Intern.* 29, 371 (1996)
5. R. Lehtiniemi and J. Hartikainen, *Rev. Sci. Instrum.* 65, 2099 (1994)
6. J. Varis, M. Oksanen, J. Rantala, and M. Luukkala, in *Review Of Progress in QNDE*, Vol. 14A, eds. D.O. Thompson and D.E. Chimenti (Plenum Press, New York, 1995), p. 511